The Astrophysical Journal, 719:958–965, 2010 August 10 doi:10.1088/0004-637X/719/1/958

MASSES OF NEUTRON STARS IN HIGH-MASS X-RAY BINARIES WITH OPTICAL ASTROMETRY

John A. Tomsick[1] and Matthew W. Muterspaugh[2,3]
[1] Space Sciences Laboratory, 7 Gauss Way, University of California, Berkeley, CA 94720-7450, USA; jtomsick@ssl.berkeley.edu
[2] Department of Mathematics and Physics, College of Arts and Sciences, Tennessee State University, Boswell Science Hall, Nashville, TN 37209, USA
[3] Tennessee State University, Center of Excellence in Information Systems, 3500 John A. Merritt Blvd., Box No. 9501, Nashville, TN 37209-1561, USA
Received 2010 May 18; accepted 2010 June 23; published 2010 July 23

ABSTRACT

Determining the type of matter that is inside a neutron star (NS) has been a long-standing goal of astrophysics. Despite this, most of the NS equations of state (EOS) that predict maximum masses in the range 1.4–2.8 $M_{\odot}$ are still viable. Most of the precise NS mass measurements that have been made to date show values close to 1.4 $M_{\odot}$, but a reliable measurement of an overmassive NS would constrain the EOS possibilities. Here, we investigate how optical astrometry at the microarcsecond level can be used to map out the orbits of High-mass X-ray Binaries (HMXBs), leading to tight constraints on NS masses. While previous studies by Unwin and coworkers and Tomsick and coworkers discuss the fact that the future *Space Interferometry Mission* should be capable of making such measurements, the current work describes detailed simulations for six HMXB systems, including predicted constraints on all orbital parameters. We find that the direct NS masses can be measured to an accuracy of ∼2.5% (1σ) in the best case (X Per), to ∼6.5% for Vela X-1, and to ∼10% for two other HMXBs.

Key words: accretion, accretion disks – astrometry – equation of state – instrumentation: interferometers – stars: individual (X Per, Vela X-1, V725 Tau, GX 301-2, SAX J0635.2+0533, V830 Cen) – stars: neutron

1. INTRODUCTION

Neutron stars (NSs) are found in a large variety of astrophysical settings, such as in accreting binaries, degenerate binaries, supernova remnants, and as isolated objects. They are one possible endpoint to the evolution of massive stars as well as being the locations of the highest magnetic field strengths and highest densities in the universe. They are often found through their radio, X-ray, or gamma-ray pulsations, which can be on timescales as short as milliseconds, and they can be accretion- or rotation-powered (Taylor et al. 1993; Bildsten et al. 1997; Abdo et al. 2009). Despite attempts to determine their fundamental properties using numerous techniques, the form of matter that exists within an NS is still a mystery.

The work that has been done to try to determine the NS composition has strong contributions from both theory and observation. For an assumed NS composition, the theoretical pressure–density relationship (i.e., equation of state; EOS) directly predicts a specific NS mass–radius relationship (Lattimer & Prakash 2001), so that measurements of mass and/or radius provide direct constraints on the NS EOS. It is currently even unknown whether NSs might be made of quark matter, which gives a radically different mass–radius relationship from normal matter (Lattimer & Prakash 2004). Most notably, each theoretical EOS has a maximum NS mass that can be supported (Lattimer & Prakash 2004), so that one measurement of an overmassive NS (∼2 $M_{\odot}$ rather than the more canonical 1.4 $M_{\odot}$) would severely constrain the possibilities for the NS EOS.

Although accurate NS mass measurements have been made for NSs in binary systems, the very accurate measurements have found values close to 1.4 $M_{\odot}$ (Thorsett & Chakrabarty 1999; Lattimer & Prakash 2007). However, more recent observations have shown evidence for overmassive NSs with best estimates in the 1.8–2.8 $M_{\odot}$ range. These have come both from High-mass X-ray Binaries (HMXBs, Barziv et al. 2001; Clark et al. 2002) and observations of binary radio pulsars (Freire et al. 2008). In addition, there is evidence from studies of "type I" X-ray bursts, which are caused by thermonuclear flashes on the NS surface (Lewin et al. 1993) that the maximum NS mass is in the 1.9–2.3 $M_{\odot}$ range (Steiner et al. 2010). Improving the mass constraints and enlarging the sample of NSs with accurate mass measurements could finally lead to definitively ruling out EOSs.

Currently, the HMXBs with the best NS mass estimates use X-ray pulsations to measure the projected size of the NS orbit and optical spectroscopy to measure the radial velocities of the companion star and, thus, to constrain the projected size of the companion's orbit (Charles & Coe 2006). However, even in cases where these measurements are possible, the binary inclination is still a major source of uncertainty in the measurement of the NS mass. Thus, in this work, we explore how NS mass measurements can be improved via optical astrometry. In many cases, HMXB orbits are as large as 20 to several hundred microarcseconds, and the companion's orbit, including the binary inclination, can be mapped directly with astrometry on the microarcsecond level (Unwin et al. 2008; Tomsick et al. 2009). Here, we look at the specific case of the future *Space Interferometry Mission* (SIM) and perform detailed simulations to determine how well this mission would be able to constrain NS masses.

2. SELECTING SOURCES FOR NEUTRON STAR MASS MEASUREMENTS

The best targets for obtaining NS mass measurements by mapping out binary orbits with optical astrometry should meet several criteria. They should be optically bright, and the angular sizes of their orbits should be large. In addition to the orbit being large, the cleanest orbital measurements will be obtained in cases where all or nearly all of the optical light comes from one of the binary components. The targets should be known to harbor NSs, and evidence for this can either come from the detection of X-ray pulsations or the presence of type I X-ray bursts. Finally, it is useful to know the orbital periods for planning the observations, and orbital periods as well as other parameters, such as the source distance and the companion mass, must be constrained in order to estimate the angular sizes of the orbits.

Table 1
Estimates of System Parameters and Astrometric Signatures

Source Name	V	d[a] (kpc)	$P_{\rm orb}$[b] (days)	$M_{\rm comp}$[c] ($M_\odot$)	$M_{\rm NS}$[d] ($M_\odot$)	ρ (μas)	$\rho_{\rm comp}$ (μas)
4U 0352+30/X Per	6.6	0.7–1.3 (1.0)	250.3	15.5[3]	1.4	1993	165.1
3A 0535+262/V725 Tau	9.6	2.0[aa]	111	8–22[4] (15)	1.4	574	49.0
XTE J1946+274	16.9	9.5	169.2	10–16[16,17] (13)	1.4	153	14.9
Vela X-1/GP Vel	6.9	1.9	8.96	23.8[7]	1.86–2.27[w,x] (2.0)	131	10.2
GX 301−2/BP Cru	10.8	3.0–4.0[bb] (3.5)	41.59	43[10]	1.85[y]	238	9.8
2S 1417−624	17.2	1.4–11.1 (6.0)	42.12	12[11]	1.4	93.7	9.8
EXO 2030+375/V2246 Cyg	19.7	7.1	46.02	17.5[19,6]	1.4	94.2	7.0
SAX J0635.2+0533	12.8	2.5–5.0 (3.8)	11.2	11–17[5,6] (14)	1.4	64.1	5.8
EXO 0331+530/BQ Cam	15.4	7	34.25	20[2]	1.4	81.8	5.4
KS 1947+300	14.2	10.0	40.4	17.5[18,6]	1.4	61.3	4.5
4U 0115+634/V635 Cas	16.3	7–8 (7.5)	24.3	18[1]	1.4	58.8	4.2
1E 1145.1−6141/V830 Cen	13.1	8	14.4	10[9]	1.4	32.6	4.0
SAX J2103.5+4545	14.2	6.5	12.68	20.0[20]	1.4	45.4	3.0
4U 1907+09	16.4	5	8.38	26–27.9[15] (27)	1.4	49.2	2.4
4U 1538−52/QV Nor	14.4	4.5–6.4 (5.5)	3.73	19.8[12,13]	1.4	23.7	1.6
XTE J1855−026	∼15	10	6.07	25[14,6]	1.4	19.4	1.0
Cen X-3/V779 Cen	13.3	9	2.09	20.2[8]	1.34[z]	9.9	0.6

Notes.
[a] The source distance given in Liu et al. 2006, and references therein. If Liu et al. 2006 give a range of values, then the value we adopt in this work is given in parentheses. If Liu et al. 2006 give multiple values, then the value we adopt comes from the literature. Superscripts indicate the following references: (*aa*) Steele et al. 1998; (*bb*) Kaper et al. 2006.
[b] From Liu et al. 2006, and references therein.
[c] The estimate for the mass of the companion star from the literature. If a paper indicates a range of values, then the value we adopt in this work is given in parentheses. Superscripts indicate the following references: (1) Negueruela & Okazaki 2001; (2) Negueruela et al. 1999; (3) Clark et al. 2001; (4) Wang & Gies 1998; (5) Kaaret et al. 1999; (6) Cox 2000; (7) Barziv et al. 2001; (8) van der Meer et al. 2007; (9) Ferrigno et al. 2008; (10) Kaper et al. 2006; (11) Okazaki & Negueruela 2001; (12) Reynolds et al. 1992; (13) Clark 2000; (14) Corbet & Mukai 2002; (15) Cox et al. 2005; (16) Verrecchia et al. 2002; (17) Wilson et al. 2003; (18) Negueruela et al. 2003; (19) Coe et al. 1988; and (20) Reig et al. 2004.
[d] We assume an NS mass of 1.4 $M_\odot$ unless there is a value given in the literature. Superscripts indicate the following references: (*w*) Barziv et al. 2001; (*x*) Quaintrell et al. 2003; (*y*) Kaper et al. 2006; (*z*) van der Meer et al. 2007.

While one could consider HMXBs and Low-mass X-ray Binaries (LMXBs), it is clear that the former will provide the best opportunities. A large number of HMXBs are bright ($V \sim$ 5–20), most of the optical light comes from the companion star, and their long orbital periods (days to a year) mean that the separation between the NS and the companion is large. In addition, many HMXBs are X-ray pulsars and for a large fraction of these the projected size of the NS orbit ($a_x \sin i$, where i is the binary inclination) has been measured, which, when combined with astrometric measurements, allows for a direct NS mass measurement.

Thus, in selecting sources, we have started with the catalog of Galactic HMXBs compiled by Liu et al. (2006). This catalog includes 114 HMXBs, including 38 sources for which both orbital periods and NS spin periods have been measured. These HMXBs range from being very bright in the optical ($V = 6$) to not having known optical counterparts, and we further cut the list down to 27 sources by requiring that the sources have a V magnitude brighter than 20. While all of these sources are known X-ray pulsars, $a_x \sin i$ has not been measured in all cases. As this parameter is required for a direct NS mass measurement, we finally select the 17 HMXBs that meet the above criteria and also have a measurement of the projected size of the NS orbit.

The 17 sources are listed in Table 1 along with their V-band magnitudes and the information relevant to estimating the angular size of the companion's orbit. If the semi-major axis of the binary is a, then the corresponding angle subtended at the source distance d is $\rho = \tan^{-1}(a/d)$, which is given by

$$\rho = 2.35\ \mu{\rm as}\ d_{\rm kpc}^{-1}\ P_{\rm orb,hr}^{2/3}(M_{\rm comp} + M_{\rm NS})^{1/3}, \quad (1)$$

where $d_{\rm kpc}$ is the distance to the source in kpc, $P_{\rm orb,hr}$ is the orbital period in hours, and $M_{\rm comp}$ and $M_{\rm NS}$ are the masses of the companion and the NS, respectively, in units of $M_\odot$. Then, the companion's orbital signature is given by $\rho_{\rm comp} = \rho M_{\rm NS}/(M_{\rm NS} + M_{\rm comp})$. In Table 1, the values of d and $P_{\rm orb}$ are taken from Liu et al. (2006). For systems where estimates of $M_{\rm NS}$ and $M_{\rm comp}$ have been given in the literature, that value is given along with the reference. Otherwise, companion masses are estimated using the spectral type (or range of spectral types) given in Liu et al. (2006) and the tables of stellar masses given in Chapter 15 of Cox (2000), and NS masses are assumed to be 1.4 $M_\odot$. If some of these systems actually contain overmassive NSs, then $\rho_{\rm comp}$ will be larger than our estimates in these cases.

3. SIMULATIONS

3.1. The Path of the HMXB Photocenter

To represent motions of the target photocenters on the sky, we define a linear coordinate system such that $x = \Delta\alpha \cos\delta$ and $y = \Delta\delta$, where α and δ are, respectively, the right ascension (R.A.) and declination (Decl.) of the sources at any time, t. The following equations represent the motion of the target photocenters:

$$x = x_0 + (t - t_0)u_x + \pi \cos\delta_\odot \sin(\alpha_\odot - \alpha_0) + x_{\rm orbital} \text{ and} \quad (2)$$

$$y = y_0 + (t - t_0)u_y + \pi \cos\delta_\odot \sin\alpha_0 \cos(\alpha_\odot - \alpha_0) + y_{\rm orbital}, \quad (3)$$

where quantities with subscript "0" are evaluated at time t_0, $\alpha_\odot$ and $\delta_\odot$ are the R.A. and Decl. for the Sun, respectively, and

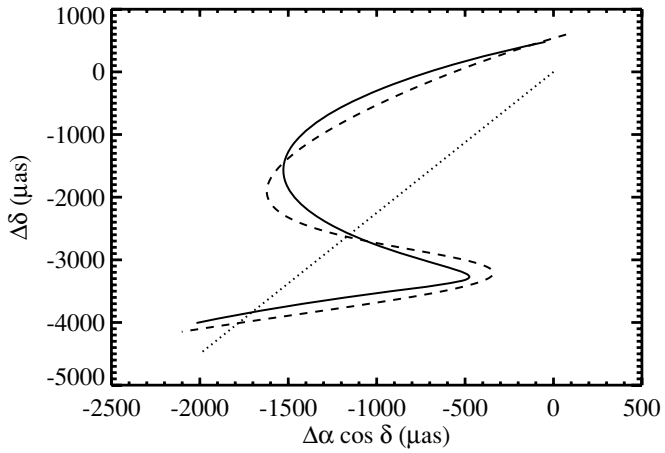

Figure 1. Best estimate for the path of the companion star and photocenter of the HMXB X Per over a period of one year. The dotted line shows the motion due only to the proper motion, and the dashed line shows the motion due to proper motion and parallax, assuming a distance of 1000 pc. The solid line includes these two effects as well as orbital motion. For X Per, the orbital period is 250 days, and we estimate that the semi-major axis of its orbit will subtend an angle of 165 μas.

$x_{\rm orbital}$ and $y_{\rm orbital}$ represent the terms in the x- and y-directions due to orbital motion. Following Lindegren (1997) and Section 2.3.4 of Volume 1 of the *Hipparcos* Catalog (Perryman et al. 1997), the orbital terms are

$$x_{\rm orbital} = BX(t) + GY(t) \text{ and } y_{\rm orbital} = AX(t) + FY(t), \quad (4)$$

where A, B, F, and G are the Thiele–Innes elements (Green 1985), which are a linearized alternative to the standard Campbell orbital elements, and depend on the angle subtended by the semi-major axis of the photocenter $\rho_{\rm phot}$, the argument of periastron ω, the position angle of the node Ω, and the binary inclination i.

The time-dependent parameters are given by

$$X(t) = \cos E - e \text{ and } Y(t) = (1 - e^2)^{1/2} \sin E, \quad (5)$$

where e is the orbital eccentricity, and E is the eccentric anomaly, which is given by

$$\frac{2\pi}{P}(t - T) = E - e \sin E, \quad (6)$$

where P is the orbital parameter, and T is the time of periastron passage.

Thus, the path of the photocenter is determined by 12 parameters: two position, two proper motion, one parallax, and seven orbital. As mentioned above, almost all of the light from an HMXB comes from the high-mass stellar companion, placing the photocenter at the location of the companion star (Coughlin et al. 2010). In the following, we make the approximation that 100% of the light comes from the companion so that $\rho_{\rm phot}$ corresponds to the semi-major axis of the companion star itself ($\rho_{\rm comp}$). Figure 1 shows the path of the companion star for the HMXB X Per over a period of one year, illustrating the different contributions to the motion.

3.2. *SIM Lite* Astrometry Measurements

Here, we consider the specific capabilities of *SIM Lite* in order to carry out our simulations. *SIM Lite* will measure positions of grid stars across the sky, which will provide global astrometric measurements to a limiting accuracy of 4 μas (1σ), and it will use reference stars around selected targets (such as the HMXBs) to provide a coordinate system covering a smaller region ($\sim 2^\circ$) where relative astrometric measurements will have a limiting accuracy of 1 μas (1σ), and these are referred to as "Narrow Angle" measurements (Nemati & Morales 2009; Unwin 2009). It is the relative uncertainty that is important for considering how accurately we will be able to measure the HMXB orbital parameters, and we use information from the *SIM Lite* project about the accuracy of these Narrow Angle measurements. However, parallax and proper motion measurements require global astrometry.

Table 2
Differential Astrometry Performance Estimator for *SIM Lite*: Input and Output

Quantity	Value
Input parameters	
Science target V magnitude	7
Science target $B - V$ color index	0.4
Characteristic reference target V magnitude	10
Characteristic reference target $B - V$ color index	0.4
Target-reference sky separation	1°
Number of reference targets	4
Number of chop cycles	4
Science target integration time per chop	30 s
Reference target integration time per chop	30 s
Output parameters	
Single measurement accuracy	1.47 μas
Science target integration time per visit	480 s
Reference target integration time per visit	480 s
Overhead time per visit	480 s
Total mission time per visit	1,440 s

In addition, for our simulations, we consider the fact that the *SIM Lite* measurements provide one-dimensional positions. While the path of the companion star is fully defined by x and y, one must consider the baseline orientation for each measurement. We use the angle θ to define the orientation of the baseline, where θ is measured from the x-axis in the counterclockwise direction. The quantity that is actually measured is the angle between the position of the target after it is projected onto the baseline and the origin of the x–y coordinate system, which is given by $r = x \cos\theta + y \sin\theta$. For the observing campaigns described below with many measurements, a baseline angle is chosen at random for each observation.

Finally, for the simulations, we determine the uncertainty in each measurement using the online *SIM Lite* "Differential Astrometry Performance Estimator" (DAPE).[4] This tool allows the user to put in information about their target as well as details about the *SIM Lite* observations, and it determines a "single-measurement accuracy" (SMA), which we use for our simulations, as well as the amount of time required for the observation. An example of the input and output from this tool is shown in Table 2. Once the SMA has been determined for a given target, a random number generator is used to select a number from a Gaussian distribution with σ equal to the SMA, and adding this number to r results in the measured angle $r_{\rm meas}$. Thus, each visit to the target generates the following information: $r_{\rm meas}$, the uncertainty in $r_{\rm meas}$, which is equal to the SMA, a timestamp (t), and a baseline angle (θ).

[4] See http://mscws4.ipac.caltech.edu/simtools_v2/.

Table 3
Comparison of Measurement Uncertainties for Vela X-1

Parameter	Description	Units	Planet Code Uncertainty[a]	New Code Uncertainty[b]
e	Eccentricity	–	± 0.04	± 0.041
i	Inclination	Degrees	± 1.14	± 1.29
ω	Argument of periastron	Degrees	± 20	± 27
t_0	Time of periastron passage	Days	± 0.5	± 0.67
Ω	Position angle of the node	Degrees	± 1	± 1.4
$\rho_{\rm comp}$	Semi-major axis	μas	± 0.2	± 0.22
d	Distance	pc	± 0.5[c]	± 0.7[c]
x_0	Reference position	arcsec	$\pm 4 \times 10^{-7}$	$\pm 5.4 \times 10^{-7}$
y_0	Reference position	arcsec	$\pm 4 \times 10^{-7}$	$\pm 5.4 \times 10^{-7}$
v_x	Proper motion	arcsec yr^{-1}	$\pm 1.1 \times 10^{-7}$	$\pm 5.2 \times 10^{-7}$
v_y	Proper motion	arcsec yr^{-1}	$\pm 1.1 \times 10^{-7}$	$\pm 5.8 \times 10^{-7}$

Notes.
[a] These are the 68% confidence (1σ) uncertainties on the Vela X-1 parameters calculated with the planet code that was written for the *SIM* Double Blind Test. These simulations include 100 observations made over five years. The observations are two-dimensional, and the SMA in each dimension is 1.27 μas.
[b] These are the 68% confidence uncertainties on the Vela X-1 parameters calculated with the new code written for this work. These simulations include 200 observations made over one year. The observations are one-dimensional, and the SMA is 1.47 μas.
[c] Although this is the error from the fit to the Narrow Angle observations, the actual uncertainty on the distance will depend on the tie-in to the absolute reference frame.

3.3. Fitting for Orbital Motion

Once the simulated data are produced, they are fitted with a function that accounts for proper motions and parallaxes for the target and reference stars as well as orbital parameters for the target. The functional form is $f = x\cos\theta + y\sin\theta$, where x and y come from Equations (2) and (3) above. In total, the equation includes 11 free parameters: five are non-orbital (x_0, y_0, u_x, u_y, and π) and six are related to the binary orbit ($\rho_{\rm comp}$, ω, Ω, i, e, and T). For the targets of interest, the orbital period is known very accurately, and we fix this parameter to the known value rather than leaving it as a free parameter.

We wrote code in Interactive Data Language (IDL) to perform the fits, and used the IDL routine *curvefit*. This routine uses the Marquardt method (Bevington & Robinson 1992), which incorporates a gradient-expansion algorithm and computes a least-squares fit. It is necessary to carry out the computations using double-precision arithmetic with stringent convergence criteria. Although *curvefit* includes an option to estimate rather than exactly compute the function derivatives for each iteration, we obtained better results when computing the exact derivatives.

3.4. Cross-check with Other Simulation Software

We checked the software described above by comparing it to the code used for simulations of *SIM Lite* observations of planets (Traub et al. 2010). The planet code was developed as part of the *SIM* Double Blind Test and uses realistic cadences and baselines but assumes two-dimensional observations. There were five teams involved in the Double Blind Test, including one team led by one of us (M.W.M.). Table 3 shows that there is, in general, excellent agreement between the two sets of code (the planet code and the new code written for this work). Although there are a couple of differences, they are easy to understand. One difference is that the proper motions are significantly more accurate for the planet code, and this is due to the fact that the simulated observations are spread over five years rather than one year. Second, the other parameters all have slightly smaller uncertainties with the planet code because the SMAs were smaller in a previous version of the DAPE calculator.

4. RESULTS

4.1. HMXBs for Simulations and Observing Parameters

Figure 2 shows the predicted orbital astrometric signatures and the V-band magnitudes for the 17 HMXBs listed in Table 1, comparing their location in the plot to the approximate sensitivity limit for *SIM Lite* taken from Tomsick et al. (2009). The limit is based on 40 hr of mission time and is conservative in the sense that it corresponds to a signal-to-noise ratio of 10. Thus, while some of the sources that are close to the limit may still have orbits that are measurable by *SIM Lite*, in this work, we focus on the six systems that are clearly above the line: X Per, V725 Tau, Vela X-1, GX 301−2, SAX J0635.2+0533, and V830 Cen.

For each of our targets, we used the DAPE tool (see above) to determine a possible plan for observing campaigns that would use 48 hr of mission time (per target). We used the parameters shown in Table 2 except for the science target V magnitude, which depends on the target, and the science target integration time per chop.[5] For the brightest four of our six targets, we were able to obtain low SMAs (<1.8 μas) with the integration time set to 30 s (see Table 4). For the fainter two targets, we increased the integration time to 60 s, giving SMAs of 2.39 and 2.66 μas for SAX J0635.2+0533 and V830 Cen, respectively. The tradeoff is having smaller numbers of observations, however, because we still use 30 s for the reference target integration time per chop and about a third of the time for the campaign is overhead (see Table 2), we only need to decrease the number of visits in the observing campaign from 120 to 90 for the fainter two targets.

While detection of orbital motion may still be possible for several of the other HMXBs close to the sensitivity line in Figure 2, such a detection is not feasible in the extreme cases. For a source as faint as EXO 2030+375 ($V = 19.7$), even if one increases the science target integration time per chop to 2 hr (the maximum allowed by the DAPE tool), the SMA is

[5] In making a measurement of an angle between sources, the *SIM Lite* instrument "chops" back and forth between the target and the reference star by changing the length of the delay line (Unwin 2009).

Table 4
Observing Parameters for a Campaign with 48 hr of Mission Time

Source Name	V	Science Target Integration Time Per Chop (s)[a]	Single Measurement Accuracy (μas)[b]	Number of Observations[c]
4U 0352+30/X Per	6.6	30	1.45	120
3A 0535+262/V725 Tau	9.6	30	1.56	120
Vela X-1/GP Vel	6.9	30	1.47	120
GX 301−2/BP Cru	10.8	30	1.76	120
SAX J0635.2+0533	12.8	60	2.39	90
1E 1145.1−6141/V830 Cen	13.1	60	2.66	90

Notes.
[a] This value was varied according to the V magnitude of the source, but the other input parameters were left at the values shown in Table 2.
[b] These values come from the DAPE for *SIM Lite*.
[c] In each case, the number of observations was adjusted to obtain a total mission time, including overheads, of 48 hr.

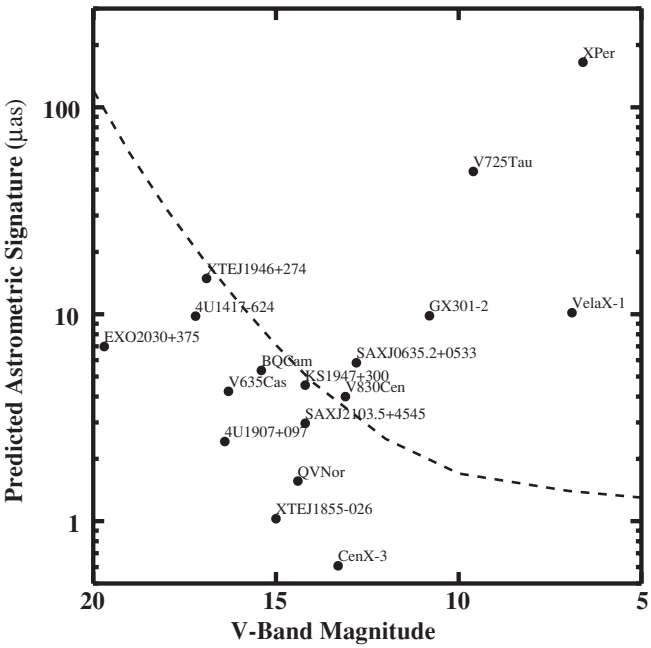

Figure 2. Predicted astrometric signatures from orbital motion vs. V-band magnitude for 17 NS HMXBs for which the projected size of the NS's orbit ($a_x \sin i$) has been measured via X-ray pulsations. The dashed line shows the threshold for detection of orbital motion in 40 hr of *SIM Lite* mission time. As described in Tomsick et al. (2009), the threshold is defined as the level at which the system's semi-major axis is 10 times larger than the astrometry noise per observation (i.e., the SMA) divided by the square root of the number of observations.

10 μas, which is larger than the 7 μas size of the orbit (see Table 1). Although one could conceivably still detect the orbit with a large number of visits, even as few as 20 visits would require nearly one month of mission time. Thus, detecting the orbit would likely take several months and would clearly not be a good use of *SIM Lite* time.

4.2. Fitting Results

For each of the six HMXBs, we simulated 2,000 *SIM Lite* observing campaigns and fitted the data with the 11 parameter model described above (note that there are 11 rather than 12 free parameters because we always fixed the orbital period to the known value). For each HMXB and each parameter, we produced histograms of the 2,000 best-fit values obtained. For all of the parameters of all of the HMXBs except for V830 Cen, the histograms appear to be normally distributed, allowing us to fit each histogram with a Gaussian and use the σ value to estimate the uncertainties on each parameter that *SIM Lite* will be able to obtain. For V830 Cen, the histogram for the eccentricity parameter is not normally distributed. We suspect that the parameter is not well constrained because V830 Cen has the smallest estimated semi-major axis, $\rho_{\rm comp} = 4.0$ μas, and we discuss the case of V830 Cen further below.

We report the simulation results for the other five HMXBs in Table 5, including the six orbital parameters as well as the parallax measurement. *SIM Lite* will greatly improve constraints on the binary inclinations, i. While the current uncertainties are on the order of $\sim 10^\circ$, with a large systematic component, *SIM Lite* will constrain i to within $\pm 0.^\circ 28$, $\pm 0.^\circ 98$, $\pm 1.^\circ 58$, and $\pm 2.^\circ 50$ for X Per, V725 Tau, Vela X-1, and GX 301−2, respectively. Also, *SIM Lite* will provide the first direct measurements of the angular size of the companion's semi-major axis, $\rho_{\rm comp}$. For example, for X Per and Vela X-1, our simulations indicate measurements of 165 ± 0.45 μas and 10.2 ± 0.28 μas.

For each HMXB, Table 5 provides a measurement of the parallax, π, and then an actual measurement of the distance. The uncertainty shown with π is that obtained from the fit to the data. However, there is also an uncertainty from the fact that the reference frame will only be known to within 4 μas, and both error components are given with the distance measurement. If X Per is at a distance of 1000 pc, we predict that *SIM Lite* will measure its distance to an accuracy of $\sim$5 pc.

For Vela X-1 and GX 301−2, the X-ray pulsation measurements (Bildsten et al. 1997) give values of e and ω that are much more accurate than our simulations predict for *SIM Lite*. Thus, we have re-fit our simulated data for these two systems and also for the two fainter sources, SAX J0635.2+0533 and V830 Cen, keeping e and ω as fixed parameters. Once this is done, the V830 Cen histograms appear to be normally distributed. Table 6 shows the fitting results for these four systems. The improvements in the constraints on the most important parameters (i, $\rho_{\rm comp}$, and d) are relatively small. The largest improvement is in the measurement of the time of periastron passage (t_0), which is expected since this parameter is related to e.

4.3. Direct Neutron Star Mass Measurements

It is possible to write an expression for the mass of an NS, $M_{\rm NS}$, in an HMXB in terms of five directly measurable quantities. Two of the quantities, $P_{\rm orb}$ and the projected linear size of the NS orbit ($a_x \sin i$), are measured by instruments

Table 5
Simulation Results and Mass Measurements (All Parameters Free)

Source Name	X Per	V725 Tau	Vela X-1	GX 301–2	SAX J0635.2+0533
			SIM Lite orbital measurements		
e	0.11 ± 0.0026	0.47 ± 0.0099	0.0898 ± 0.050	0.462 ± 0.068	0.29 ± 0.15
i (°)	29.82 ± 0.28	30.50 ± 0.98	82.52 ± 1.58	67.40 ± 2.50	49.12 ± 7.84
ω (°)	108 ± 1.5	310 ± 2.2	332.59 ± 33.6	130.4 ± 8.2	356 ± 36
t_0 (days)	± 0.99	± 0.33	± 0.84	± 0.84	± 0.88
Ω (°)	45 ± 0.5	45 ± 2.0	45 ± 1.6	45 ± 2.7	45 ± 12
$\rho_{\rm comp}$ (μas)	165 ± 0.45	49.0 ± 0.41	10.2 ± 0.28	9.8 ± 0.49	5.8 ± 0.56
			SIM Lite distance measurement		
π (μas)	1000 ± 0.87	500 ± 0.37	526 ± 0.28	278 ± 0.31	263 ± 0.68
d (pc)	1000(± 0.87)(± 4)	2000(± 1.5)(± 16)	1900(± 1.0)(± 14)	3500(± 4.0)(± 52)	3800(± 9.9)(± 58)
			X-ray measurement of the projected size of the pulsar's orbit		
$a_x \sin i$ (lt-s)[a]	454.0 ± 4.0[1]	267 ± 13[2]	113.89 ± 0.13[2]	368.3 ± 3.7[2]	83 ± 11[3]
			Derived NS mass measurement and error contributions		
$M_{\rm NS}$ ($M_\odot$)	1.40 ± 0.035	1.40 ± 0.15	2.00 ± 0.13	1.85 ± 0.21	1.40 ± 0.59
$\delta M_{\rm NS,distance}$ ($M_\odot$)	0.008	0.014	0.018	0.032	0.029
$\delta M_{{\rm NS},\rho_{\rm comp}}$ ($M_\odot$)	0.004	0.014	0.062	0.103	0.156
$\delta M_{{\rm NS},i}$ ($M_\odot$)	0.025	0.087	0.110	0.176	0.463
$\delta M_{{\rm NS},a_x \sin i}$ ($M_\odot$)	0.023	0.125	0.004	0.036	0.329

Note. [a] These are from the following: (1) Delgado-Martí et al. 2001; (2) Bildsten et al. 1997; (3) Kaaret et al. 2000.

Table 6
Simulation Results and Mass Measurements (e and ω fixed)

Source Name	Vela X-1	GX 301−2	SAX J0635.2+0533	V830 Cen
		SIM Lite orbital measurements		
e	0.0898[a]	0.462[a]	0.29[a]	0.20[a]
i (°)	82.52 ± 1.55	67.40 ± 2.29	49.12 ± 7.78	60.68 ± 9.87
ω (°)	332.59[a]	130.4[a]	356[a]	128[a]
t_0 (days)	± 0.040	± 0.27	± 0.31	± 0.47
Ω (°)	45 ± 1.6	45 ± 2.4	45 ± 10	45 ± 13
$\rho_{\rm comp}$ (μas)	10.2 ± 0.27	9.8 ± 0.37	5.8 ± 0.52	4.0 ± 0.56
		SIM Lite distance measurement		
π (μas)	526 ± 0.27	278 ± 0.31	263 ± 0.67	125 ± 0.51
d (pc)	1900(± 1.0)(± 14)	3500(± 4.0)(± 52)	3800(± 9.7)(± 58)	8000(± 33)(± 256)
		Derived neutron star mass measurement and error contributions[b]		
$M_{\rm NS}$ ($M_\odot$)	2.00 ± 0.13	1.85 ± 0.19	1.40 ± 0.59	1.40 ± 0.57
$\delta M_{\rm NS,distance}$ ($M_\odot$)	0.018	0.032	0.029	0.062
$\delta M_{{\rm NS},\rho_{\rm comp}}$ ($M_\odot$)	0.061	0.078	0.145	0.242
$\delta M_{{\rm NS},i}$ ($M_\odot$)	0.108	0.161	0.463	0.516
$\delta M_{{\rm NS},a_x \sin i}$ ($M_\odot$)	0.004	0.036	0.329	0.044

Notes.
[a] Fixed.
[b] The value of $a_x \sin i$ used for V830 Cen is 99.4 ± 1.8 lt-s (Ray & Chakrabarty 2002). The values used for the other sources are the same as in Table 5.

other than *SIM Lite*. The other three quantities, $\rho_{\rm comp}$, i, and d; will be measured by *SIM Lite* as described above. Starting from the standard orbital equations that are typically used for measurements of the components of binary systems (e.g., Equation (5.3) in Charles & Coe 2006), we derive the following equation:

$$M_{\rm NS} = \frac{4\pi^2}{G P_{\rm orb}} \frac{d \tan \rho_{\rm comp}}{\sin^2 i} [(a_x \sin i) + d \tan \rho_{\rm comp} \sin i]^2, \quad (7)$$

where $M_{\rm NS}$, $P_{\rm orb}$, d, and $a_x \sin i$ are in the same units as the gravitational constant, G, e.g., CGS units, and i and $\rho_{\rm comp}$ are angles. For X-ray pulsars, the projected size of the NS orbit can often be determined to very high accuracy, e.g., $a_x \sin i = 113.89 \pm 0.13$ lt-s for Vela X-1 (Bildsten et al. 1997). By obtaining long (years) time baseline X-ray or optical observations, X-ray pulsar orbital periods are, for our purposes, known with negligible uncertainties.

In addition to the *SIM Lite*-measured parameters in the top parts of Table 5, the values of $a_x \sin i$ are given for the five HMXB systems, and this, in turn, is used to calculate $M_{\rm NS}$. For X Per, our simulations predict that *SIM Lite* will measure the NS mass to ∼2.5% ($M_{\rm NS} = 1.40 \pm 0.035$ $M_\odot$, where the uncertainty corresponds to the 68% (1σ) confidence level).

The second-best measurement would be obtained for Vela X-1, for which we predict a ∼6.5% uncertainty on $M_{\rm NS}$. It should be noted that these values consider both components (from the fit and from the reference frame) of the distance uncertainty. For each HMXB, the contribution from each parameter (d, $\rho_{\rm comp}$, i, and $a_x \sin i$) to the uncertainty on $M_{\rm NS}$ is given in Tables 5 and 6. For V725 Tau, the largest contribution to the uncertainty comes from the $a_x \sin i$ term, so that the future measurement of $M_{\rm NS}$ can be substantially improved with X-ray observations of this system.

5. DISCUSSION AND CONCLUSIONS

The results of these simulations show that *SIM Lite* will provide excellent constraints on the masses of NSs in HMXBs. There is currently no direct method for obtaining the binary inclinations (i) of HMXBs, and this will be a major improvement in the measurements. This is especially true for non-eclipsing systems like X Per and V725 Tau, for which i is thought to be near 30°, but it is currently only estimated to about ±10°–15°. With such a large uncertainty in i, we do not have any current estimate of the NS masses in these systems, which is why we assume 1.4 $M_\odot$ for the simulations. Since these are both accreting systems, there is a strong possibility that the NS masses are significantly higher, which could allow for a constraint on the NS EOS.

The current constraints on i are better for Vela X-1, which is an eclipsing system, but HMXBs with relatively short orbital periods can be eclipsing for a wide range of inclinations; thus, the improvement in the measurement of i that *SIM Lite* will provide is important. There are already suggestions that the Vela X-1 NS is overmassive, and if *SIM Lite* finds that the NS mass is, e.g., 2.00 ± 0.13 $M_\odot$, as found with our simulations, this would rule out many NS EOSs (Lattimer & Prakash 2004).

There are also possibilities for further improvements to the accuracy of the NS mass measurements estimated in Tables 5 and 6. We assume in our simulations that we will use *SIM Lite* to determine the times of periastron (t_0), but if contemporaneous X-ray observations can be made, it will be possible to accurately determine this time using the X-ray pulsations. Also, we find that, after *SIM Lite* measurements of V725 Tau, the uncertainty in $M_{\rm NS}$ will be dominated by the measurement of $a_x \sin i$; thus, X-ray measurements to improve the measurement of this parameter could ultimately lead to a mass constraint that is nearly as good as that for X Per. Finally, one more piece of information that we have not considered in this work is the radial velocity semi-amplitude of the companion star ($K_{\rm comp}$). This parameter is related to the projected size of the orbit, and a cross-check between this parameter and the astrometric parameters ($\rho_{\rm comp}$, d, i, and e) will be possible (e.g., Pourbaix & Jorissen 2000).

Although we focus on obtaining NS masses via orbital measurements in this work, it should also be pointed out that *SIM Lite* can also contribute to constraining EOSs by improving measurements of NS radii. Two techniques for measuring the radii of NSs in LMXBs use measurements of the X-ray emission from the NS surface: one is to observe the thermal X-rays from the surface of an NS when the accretion rate is very low (e.g., Rutledge et al. 2002), and another is to measure the thermal emission near the end of a type I X-ray burst (Galloway et al. 2008; Özel et al. 2010). In both cases, the distance to the LMXB is the largest uncertainty in the NS radius measurement (see the references above and Tomsick et al. 2009), and *SIM Lite* will provide accurate distances for a large number of LMXBs.

Finally, it is important to note that our requirement in this work that $a_x \sin i$ be a measured parameter eliminates many interesting HMXBs that will be excellent targets for *SIM Lite*. In Tomsick et al. (2009), we find ∼20 HMXBs for which the predicted astrometric signatures will be large enough for orbital measurements. This includes well-known sources such as the black hole system Cyg X-1 (Caballero-Nieves et al. 2009) and the likely black hole system SS 433 (Blundell, et al. 2008) as well as systems where it is not clear whether the compact object is a black hole or an NS. These include the interesting case of 4U 1700–377, which is thought to be an NS based on its X-ray properties, but which has a compact object mass estimated at 2.4 $M_\odot$. Also, precise compact object masses have not been determined for the gamma-ray binaries LS I +61° 303 and LS 5039 (Dubus 2006), but given that there are only a small number of high-mass binaries known to produce gamma-ray emission, determining the type of compact object in these systems is of great interest.

This work was sponsored in part by the National Aeronautics and Space Administration (NASA) through a contract with the Jet Propulsion Laboratory, California Institute of Technology. M.W.M. acknowledges support from the Townes Fellowship Program and the State of Tennessee Center of Excellence program. The *SIM* planet-finding code was developed as part of the *SIM* Double Blind Test with support from NASA contract NAS7-03001 (JPL 1336910). J.A.T. acknowledges useful communications with Valeri Makarov about the planned operation of *SIM Lite* in narrow-angle mode. J.A.T. acknowledges useful discussions with Sabine Reffert, Andreas Quirrenbach, Stuart Shaklan, Xiaopei Pan, and Shri Kulkarni.

REFERENCES

Abdo, A. A., et al. 2009, Science, 326, 1512
Barziv, O., Kaper, L., Van Kerkwijk, M. H., Telting, J. H., & Van Paradijs, J. 2001, A&A, 377, 925
Bevington, P. R., & Robinson, D. K. 1992, Data Reduction and Error Analysis for the Physical Sciences (2nd ed.; New York: McGraw-Hill)
Bildsten, L., et al. 1997, ApJS, 113, 367
Blundell, K. M., Bowler, M. G., & Schmidtobreick, L. 2008, ApJ, 678, L47
Caballero-Nieves, S. M., et al. 2009, ApJ, 701, 1895
Charles, P. A., & Coe, M. J. 2006, Optical, Ultraviolet and Infrared Observations of X-ray Binaries, in Compact Stellar X-ray Sources, ed. W. Lewin & M. van der Klis (Cambridge: Cambridge Univ. Press), 215
Clark, G. W. 2000, ApJ, 542, L131
Clark, J. S., Goodwin, S. P., Crowther, P. A., Kaper, L., Fairbairn, M., Langer, N., & Brocksopp, C. 2002, A&A, 392, 909
Clark, J. S., Tarasov, A. E., Okazaki, A. T., Roche, P., & Lyuty, V. M. 2001, A&A, 380, 615
Coe, M. J., Payne, B. J., Longmore, A., & Hanson, C. G. 1988, MNRAS, 232, 865
Corbet, R. H. D., & Mukai, K. 2002, ApJ, 577, 923
Coughlin, J. L., et al. 2010, ApJ, 717, 776
Cox, A. N. (ed.) 2000, in Allen's Astrophysical Quantities (4th ed.; Melville, NY: AIP)
Cox, N. L. J., Kaper, L., & Mokiem, M. R. 2005, A&A, 436, 661
Delgado-Martí, H., Levine, A. M., Pfahl, E., & Rappaport, S. A. 2001, ApJ, 546, 455
Dubus, G. 2006, A&A, 456, 801
Ferrigno, C., Segreto, A., Mineo, T., Santangelo, A., & Staubert, R. 2008, A&A, 479, 533
Freire, P. C. C., Wolszczan, A., van den Berg, M., & Hessels, J. W. T. 2008, ApJ, 679, 1433
Galloway, D. K., Özel, F., & Psaltis, D. 2008, MNRAS, 387, 268
Green, R. M. 1985, Spherical Astronomy (Cambridge: Cambridge Univ. Press), 470
Kaaret, P., Cusumano, G., & Sacco, B. 2000, ApJ, 542, L41
Kaaret, P., Piraino, S., Halpern, J., & Eracleous, M. 1999, ApJ, 523, 197
Kaper, L., van der Meer, A., & Najarro, F. 2006, A&A, 457, 595

Lattimer, J. M., & Prakash, M. 2001, ApJ, 550, 426
Lattimer, J. M., & Prakash, M. 2004, Science, 304, 536
Lattimer, J. M., & Prakash, M. 2007, Phys. Rep., 442, 109
Lewin, W. H. G., van Paradijs, J., & Taam, R. E. 1993, Space Sci. Rev., 62, 223
Lindegren, L. 1997, in Proc. ESA Symp., Hipparcos '97, ed. M. A. C. Perryman, P. L. Bernacca, & B. Battrick (ESA SP-402; Noordwijk: ESA), 13
Liu, Q. Z., van Paradijs, J., & van den Heuvel, E. P. J. 2006, A&A, 455, 1165
Negueruela, I., Israel, G. L., Marco, A., Norton, A. J., & Speziali, R. 2003, A&A, 397, 739
Negueruela, I., & Okazaki, A. T. 2001, A&A, 369, 108
Negueruela, I., Roche, P., Fabregat, J., & Coe, M. J. 1999, MNRAS, 307, 695
Nemati, B., & Morales, M. J. 2009, in The Astrometric Error Budget, SIM Lite Astronomical Observatory, ed. J. Davidson et al. (Pasadena, CA: NASA JPL), 183
Okazaki, A. T., & Negueruela, I. 2001, A&A, 377, 161
Özel, F., Baym, G., & Guver, T. 2010, submitted to PRL (arXiv:1002.3153)
Perryman, M. A. C., et al. 1997, A&A, 323, L49
Pourbaix, D., & Jorissen, A. 2000, A&AS, 145, 161
Quaintrell, H., Norton, A. J., Ash, T. D. C., Roche, P., Willems, B., Bedding, T. R., Baldry, I. K., & Fender, R. P. 2003, A&A, 401, 313
Ray, P. S., & Chakrabarty, D. 2002, ApJ, 581, 1293
Reig, P., Negueruela, I., Fabregat, J., Chato, R., Blay, P., & Mavromatakis, F. 2004, A&A, 421, 673
Reynolds, A. P., Bell, S. A., & Hilditch, R. W. 1992, MNRAS, 256, 631
Rutledge, R. E., Bildsten, L., Brown, E. F., Pavlov, G. G., Zavlin, V. E., & Ushomirsky, G. 2002, ApJ, 580, 413
Steele, I. A., Negueruela, I., Coe, M. J., & Roche, P. 1998, MNRAS, 297, L5
Steiner, A. W., Lattimer, J. M., & Brown, E. F. 2010, arXiv:1005.0811
Taylor, J. H., Manchester, R. N., & Lyne, A. G. 1993, ApJS, 88, 529
Thorsett, S. E., & Chakrabarty, D. 1999, ApJ, 512, 288
Tomsick, J. A., Shaklan, S. B., & Pan, X. 2009, in Black Holes and Neutron Stars, SIM Lite Astronomical Observatory, ed. J. Davidson et al. (Pasadena, CA: NASA JPL), 97
Traub, W. A., et al. 2010, in Extrasolar Planets in Multi-Body Systems: Theory and Observations (EAS Pub. Ser. 42), ed. K. Goździewski, A. Niedzielski, & J. Schneider (Les Ulis: EDP), 191
Unwin, S. C. 2009, in Observing with SIM Lite, SIM Lite Astronomical Observatory, ed. J. Davidson et al. (Pasadena, CA: NASA JPL), 173
Unwin, S. C., et al. 2008, PASP, 120, 38
van der Meer, A., Kaper, L., van Kerkwijk, M. H., Heemskerk, M. H. M., & van den Heuvel, E. P. J. 2007, A&A, 473, 523
Verrecchia, F., et al. 2002, A&A, 393, 983
Wang, Z. X., & Gies, D. R. 1998, PASP, 110, 1310
Wilson, C. A., Finger, M. H., Coe, M. J., & Negueruela, I. 2003, ApJ, 584, 996